

## ***Supplementary information for:***

# **Studying the significance of the parameters involved in the synthesis of Y-UiO-66 to improve product yield**

Micaela Richezzi,<sup>a</sup> P. Rafael Donnarumma,<sup>b</sup> Ashlee J. Howarth<sup>\*a</sup>

<sup>a</sup> Department of Chemistry and Biochemistry and Centre for NanoScience Research, Concordia University, 7141 Sherbrooke Street West, Montreal, Quebec, H4B 1R6, Canada

<sup>b</sup> CIC biomaGUNE, Parque Científico y Tecnológico de Gipuzkoa, Paseo Miramón 194, 20014, Donostia/San Sebastián, Gipuzkoa, Spain.

*Rare-earth, MOFs, RE-MOFs, Yttrium, Design of experiments*

## **Materials**

All solvents and reagents were purchased from commercial sources. N,N-dimethylformamide (DMF), N,N-dimethylacetamide (DMAc), acetone, and nitric acid (70%) were purchased from Fisher Scientific (Fisher Chemical).  $Y(NO_3)_3 \cdot xH_2O$  and  $Tb(NO_3)_3 \cdot xH_2O$  were purchased from Thermo Scientific,  $Ho(NO_3)_3 \cdot xH_2O$  and  $Yb(NO_3)_3 \cdot xH_2O$ , were purchased from Chemicals 101. 2,6-difluorobenzoic acid (2,6-DFBA) was purchased from Ambeed. Terephthalic acid (BDC) was purchased from Acros Organics.

Note: 2,6-dFBA was purified by dissolving in acetone (10 g in 20 mL), filtering the impurities and letting the acetone evaporate at room temperature. Not purifying this reagent or doing it with a different procedure might impact the reproducibility of the synthesis of the MOFs herein reported.

## **Instrumentation**

Powder X-ray diffraction (PXRD) patterns were obtained using a Rigaku MiniFlex diffractometer (measurements made over a range of  $3^\circ < 2\theta < 40^\circ$  with a 0.100 °/s scanning speed). Neat samples were smeared onto a zero-background sample holder. Data were collected using a continuous coupled  $\theta/2\theta$  scan with Ni-filtered  $CuK\alpha$  ( $\lambda = 1.54178 \text{ \AA}$ ).

Thermogravimetric analysis (TGA) was carried out using a Mettler Toledo TGA/DSC 3+ equipped with an SDTA sensor, small furnace, and XP1 balance from room temperature to 800 °C at a rate of 10 °C/min under air.

Samples for nitrogen adsorption/desorption were activated using a Micromeritics Smart VacPrep instrument equipped with a hybrid turbo vacuum pump. Nitrogen adsorption-desorption isotherms were measured at 77 K on a Micromeritics TriStar II Plus instrument. Activation of all RE-UiO-66 samples was performed at 80 °C for 20 h.

$^1H$ -NMR spectra were recorded on a 300 MHz Bruker spectrometer and the chemical shifts were referenced to the residual solvent peaks. Samples were digested using  $D_2SO_4$  (12 drops) and then dissolved in  $DMSO-d_6$  (0.65 mL).

Scanning electron microscopy (SEM) micrographs were collected on a Phenom ProX desktop SEM. Samples were dispersed on a carbon taped aluminium stub, coated with 5 nm of Au and placed

on a charge reducing sample holder. SEM images were collected at accelerating voltage of 10 kV and magnification of 1350x and 3800x.

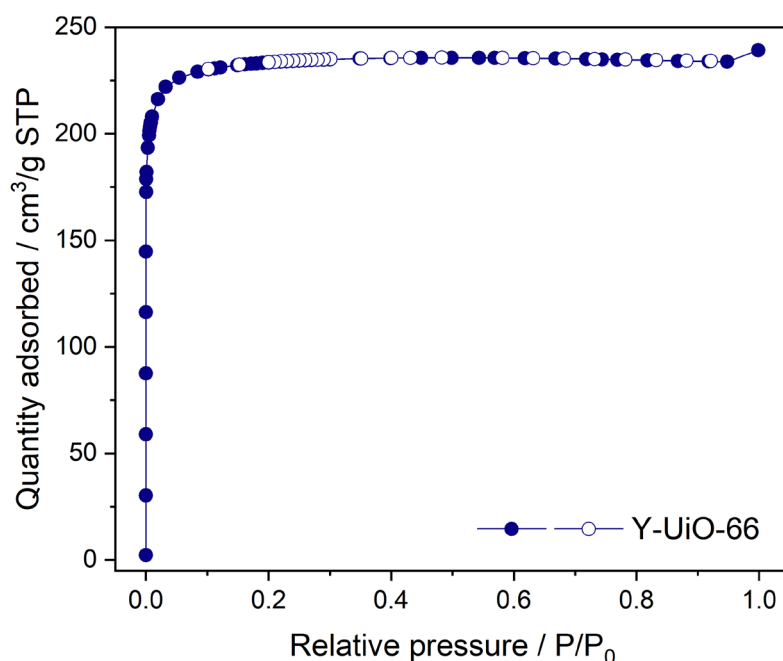
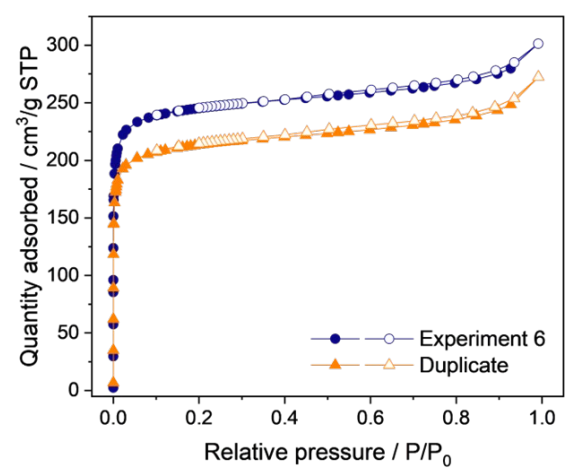
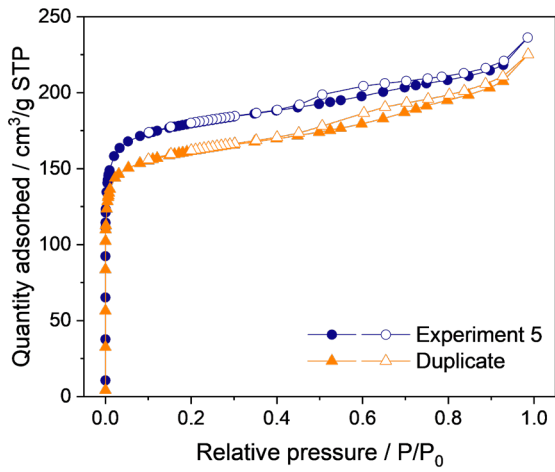
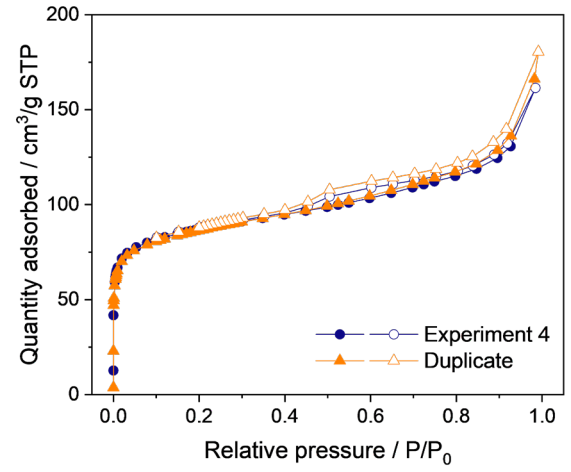
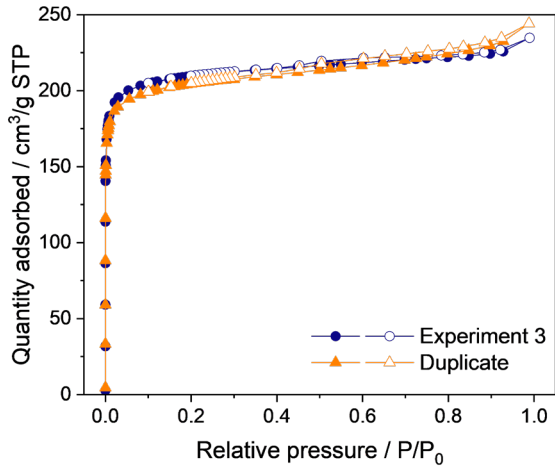
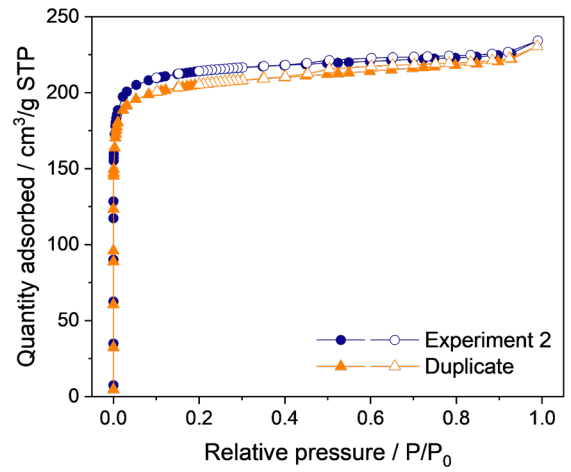
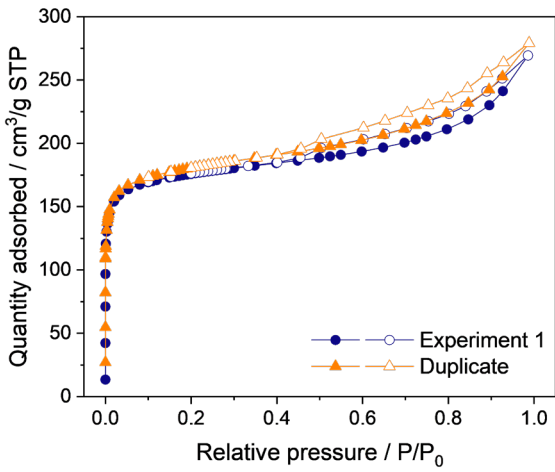
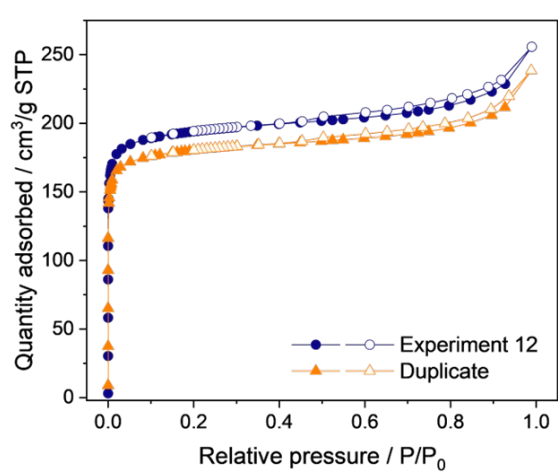
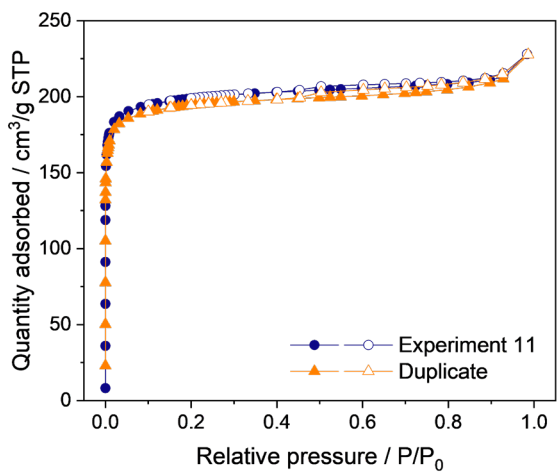
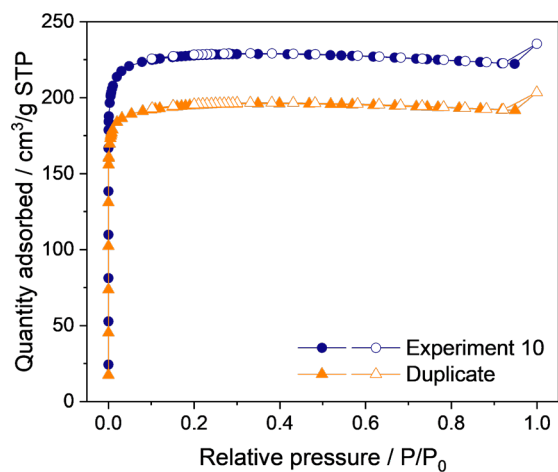
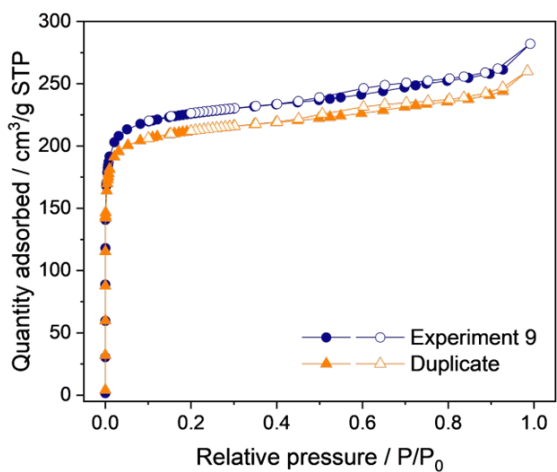
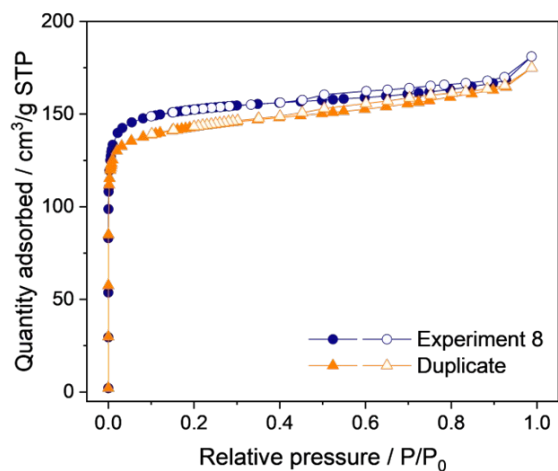
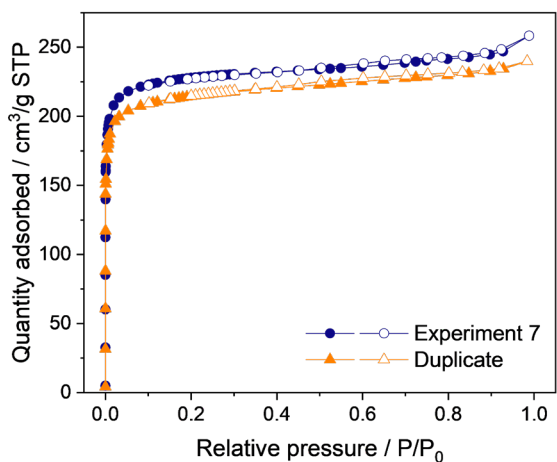


Figure S1 N<sub>2</sub> adsorption-desorption isotherm of Y-UiO-66 obtained using the reported procedure, presenting a surface area of 940 m<sup>2</sup>/g. Closed circles correspond to adsorption and open correspond to desorption.

Table S1 Yields and surface areas obtained for the 16 experiments and their duplicates.

Experiment	Temperature	Modulator	Linker	Time	Co-modulator	Water	Solvent	Original			Duplicate		
								Yield (mg)	Yield (%)	Surface area (m <sup>2</sup> /g)	Yield (mg)	Yield (%)	Surface area (m <sup>2</sup> /g)
1	1	1	-1	-1	-1	-1	1	33.4	67	675	35.1	70	686
2	-1	-1	1	1	1	1	-1	33.6	67	850	39.8	80	814
3	1	1	1	-1	1	-1	-1	32.2	64	832	38.9	78	809
4	1	1	-1	1	-1	1	-1	28.5	57	326	25.0	50	311
5	1	-1	-1	1	1	-1	-1	31.5	63	699	34.1	68	622
6	-1	1	1	1	-1	-1	-1	36.3	73	968	31.4	63	837
7	-1	-1	-1	1	-1	1	1	35.3	71	907	31.1	62	850
8	1	1	1	1	1	1	1	33.8	68	605	36.2	72	566
9	-1	1	-1	1	1	-1	1	38.0	76	889	37.0	74	834
10	-1	-1	1	-1	1	-1	1	19.0	38	920	21.7	43	789
11	1	-1	1	-1	-1	1	-1	34.7	69	792	34.9	70	770
12	1	-1	-1	-1	1	1	1	36.0	72	770	35.8	72	716
13	-1	1	-1	-1	1	1	-1	23.9	48	1033	19.8	40	1177
14	-1	-1	-1	-1	-1	-1	-1	20.8	42	1033	23.4	47	1069
15	1	-1	1	1	-1	-1	1	29.6	59	668	32.5	65	533
16	-1	1	1	-1	-1	1	1	35.9	72	946	34.1	68	880





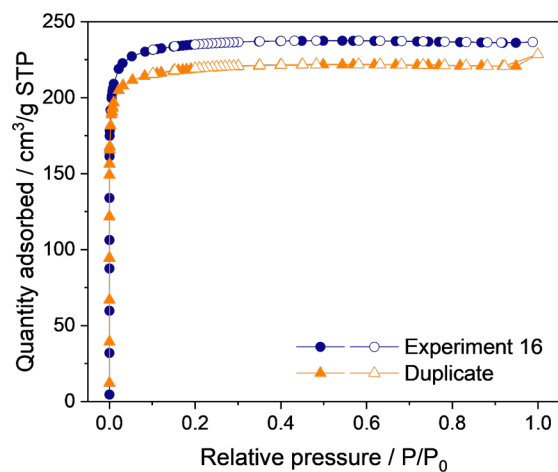
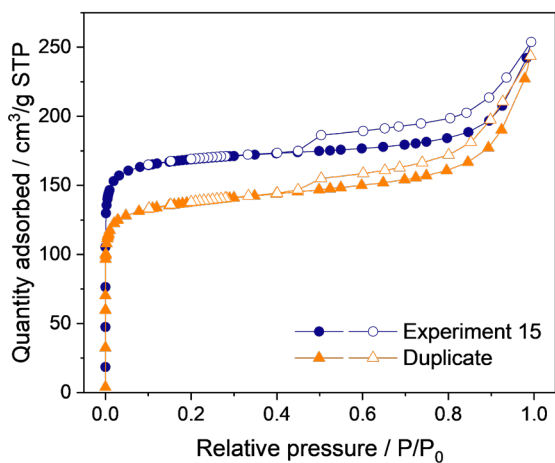
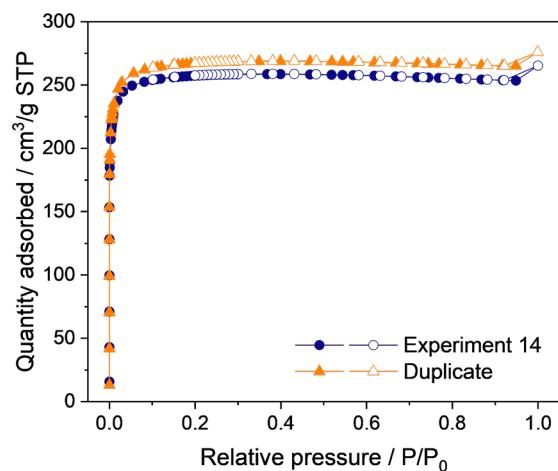
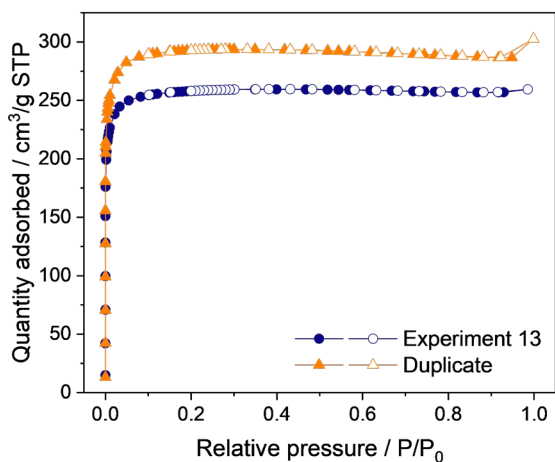


Figure S2 N<sub>2</sub> adsorption-desorption isotherms of Y-UiO-66 samples obtained from the 16 experiments of the DoE. Closed circles and triangles correspond to adsorption and open correspond to desorption.

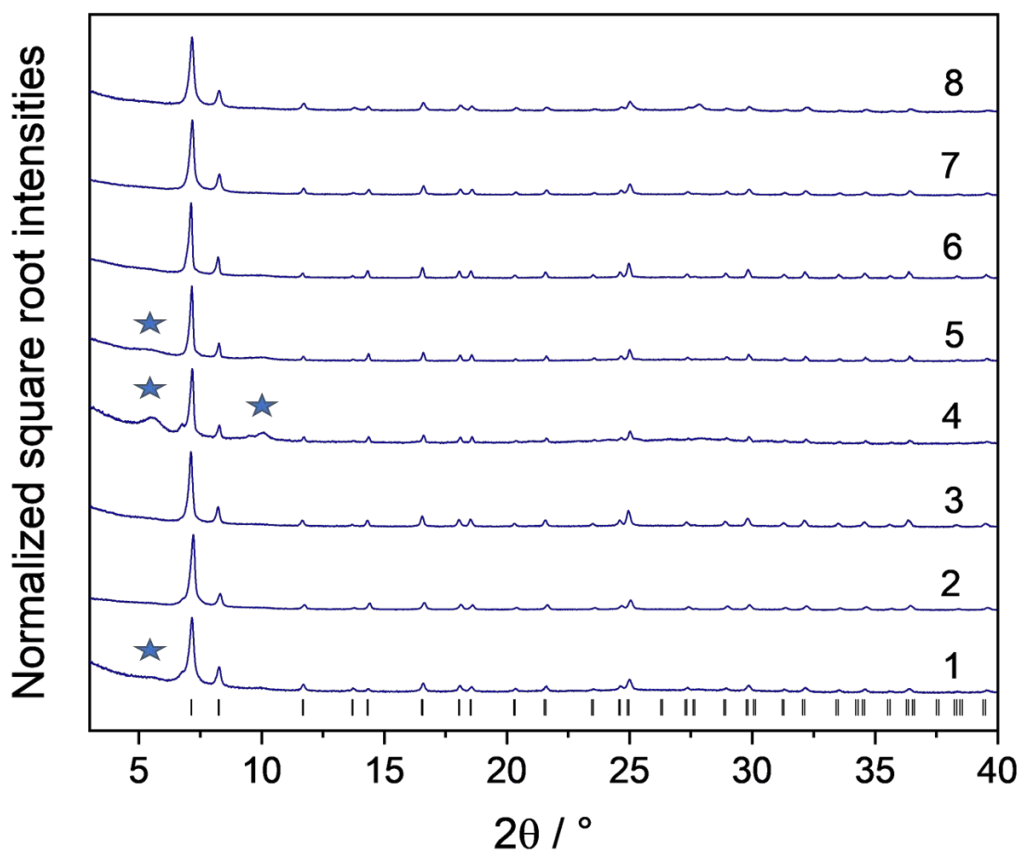
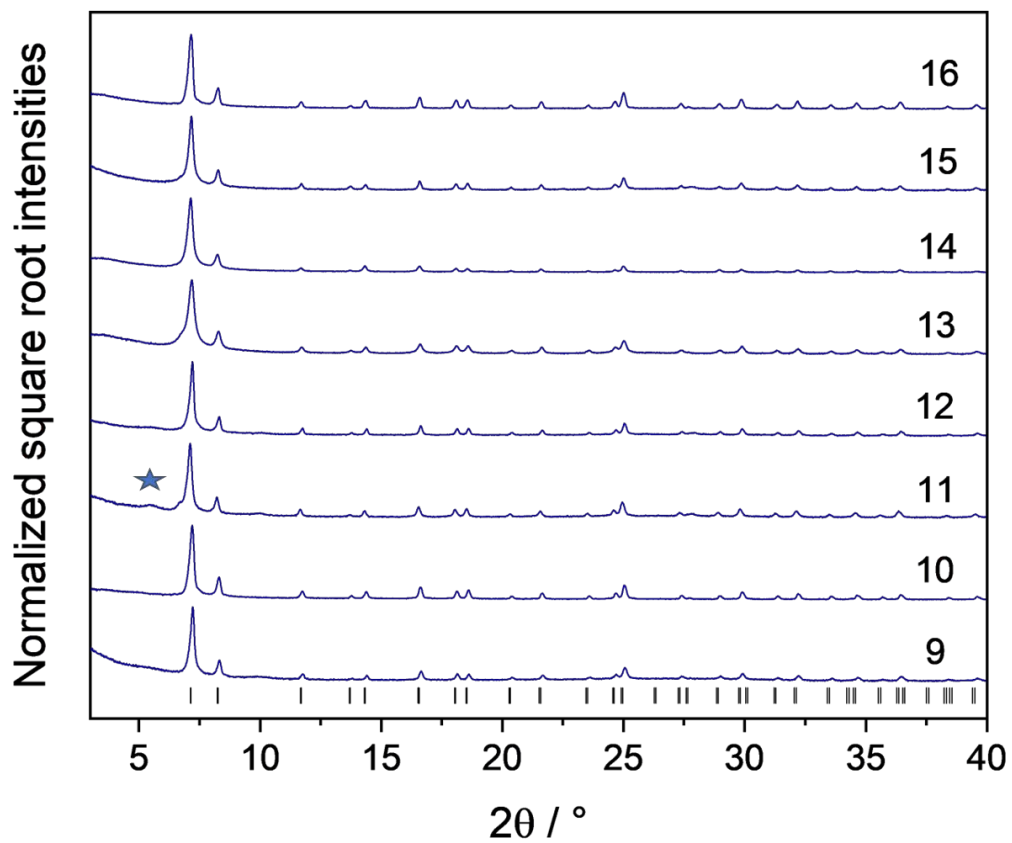


Figure S3 PXRD patterns of Y-UiO-66 samples obtained from the 16 experiments of the DoE. Stars indicate the peaks that do not correspond to allowed reflections (vertical bars).

In an attempt to identify the impurities leading to additional reflections in the PXRD patterns in Figure S3, the product of reaction #4 was digested in  $D_2SO_4$  and  $DMSO-d_6$  for  $^1H$  NMR spectroscopy. The  $^1H$  NMR spectrum (Figure S4) shows a small organic impurity at 2.3ppm, which is discussed in the main text on page 3 and can be removed by washing with MeOH. On one hand, it has been shown by Balkus et al.<sup>1</sup> that the reaction of RE metals with fluorinated modulators can give the corresponding  $REF_3$  (peaks between 24 and 30  $^{\circ}2\theta$ ), sometimes layered with hydroxide (in this case, the peak around 5  $^{\circ}2\theta$  is observed). All the reactions that presented additional peaks in the PXRD patterns (Figure S3) were performed at 130  $^{\circ}C$ , indicating that the high temperature might play a role in favouring the formation of this  $REF_3$ , layered with hydroxide, phase. We repeated reaction #4 without adding the linker and obtained  $YF_3$  (Figure S5) confirming the identity of the impurity peaks.

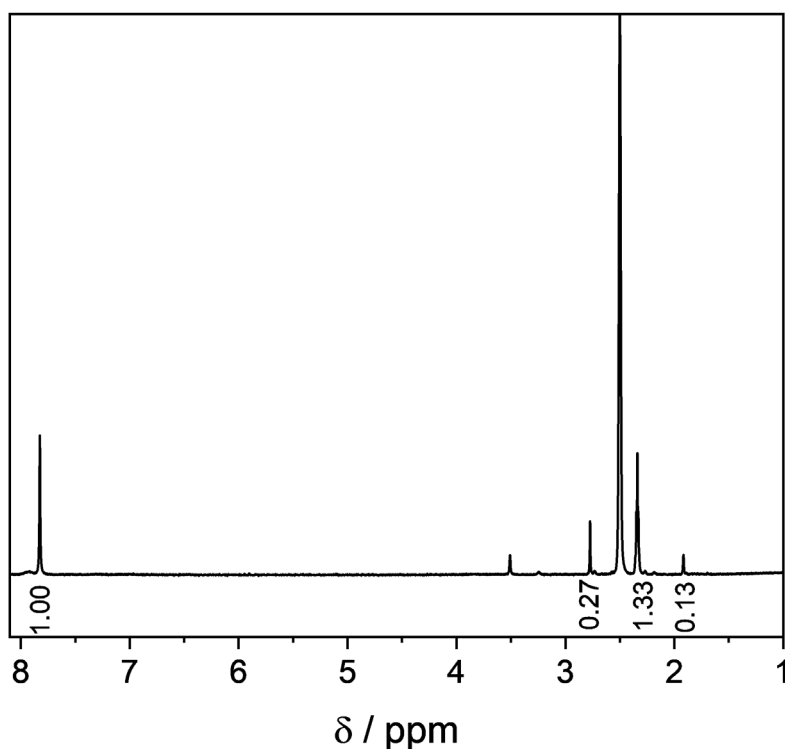


Figure S4  $^1H$  NMR spectrum of Y-UiO-66 obtained with reaction #4.

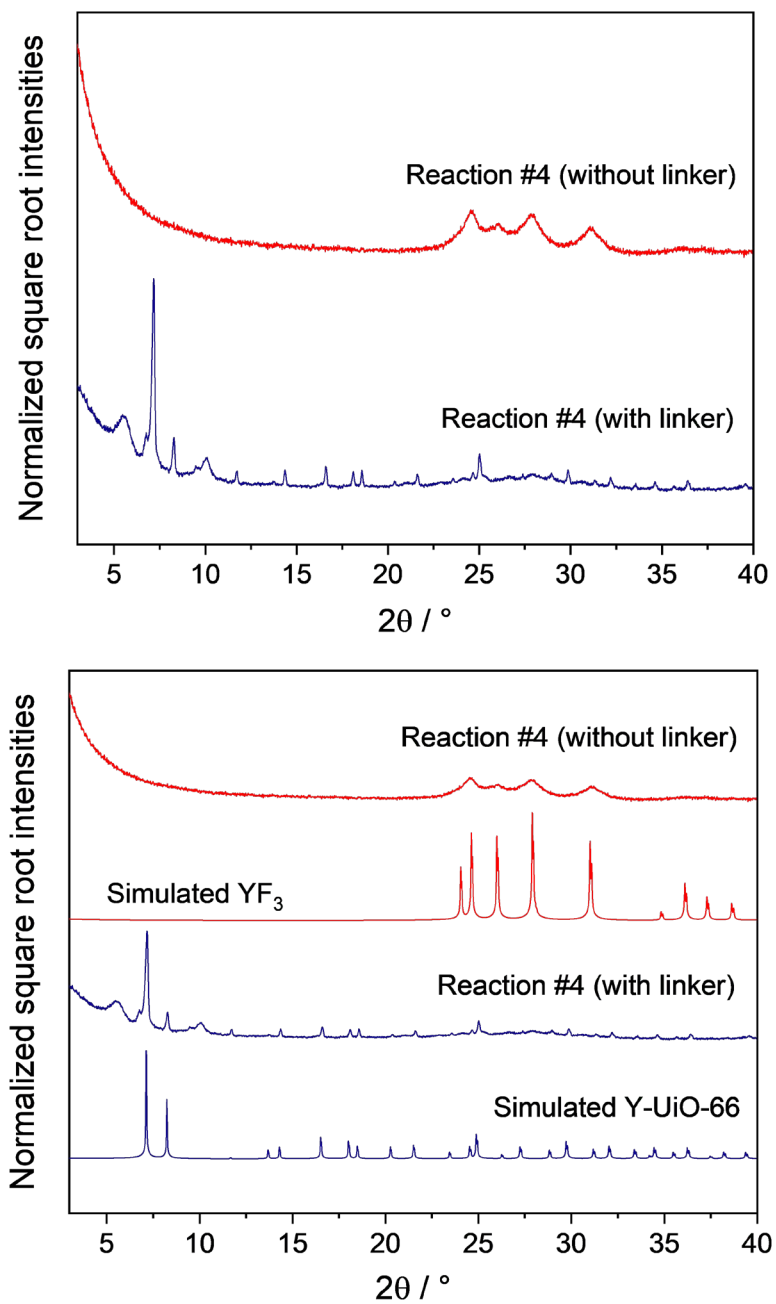


Figure S5 PXRD patterns of reaction #4 with and without linker, and the simulated pattern for Y-Uio-66 and YF<sub>3</sub> (ICSD 26595).

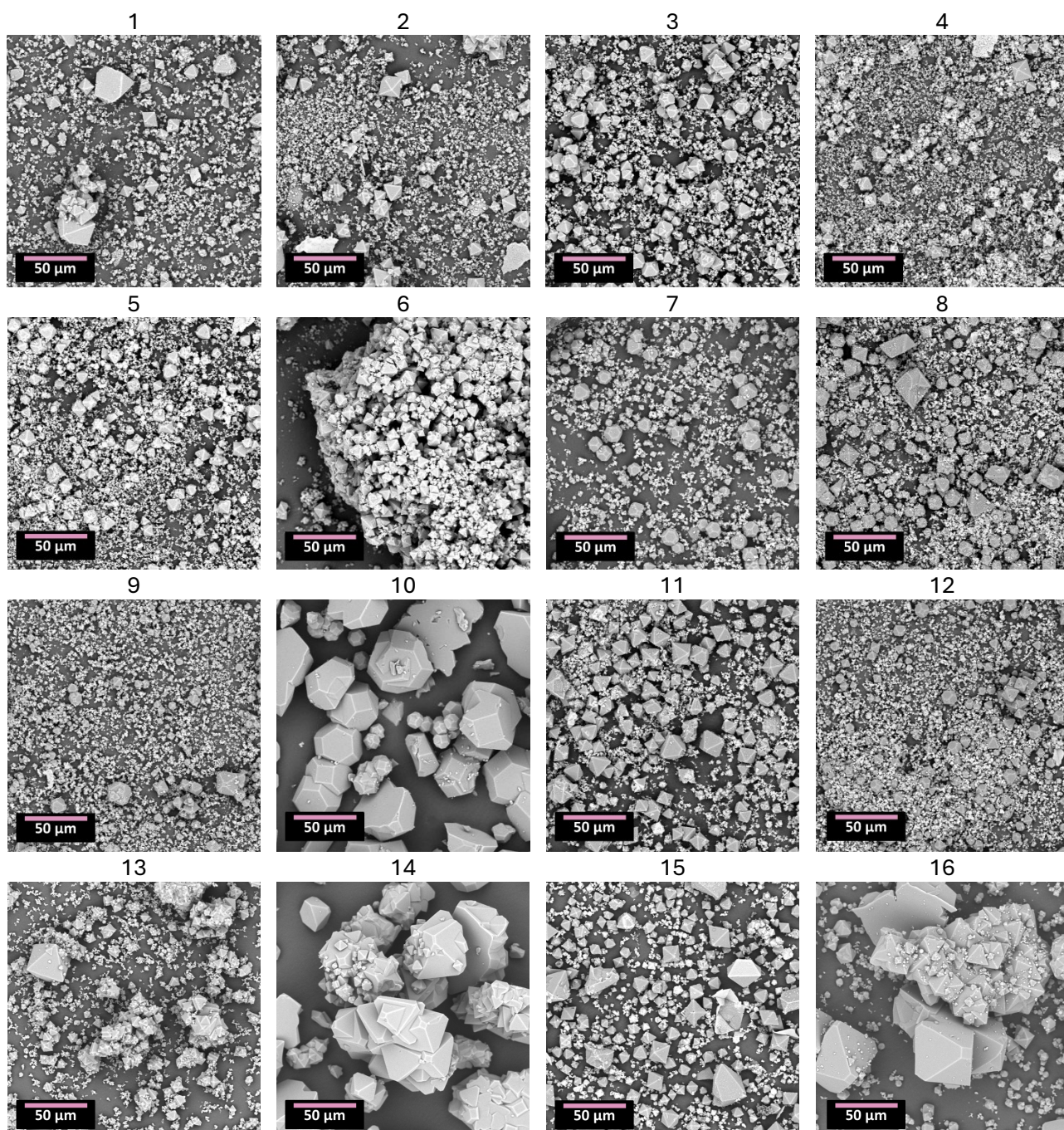


Figure S6 SEM images of Y-Uio-66 samples obtained from the 16 experiments of the DoE.

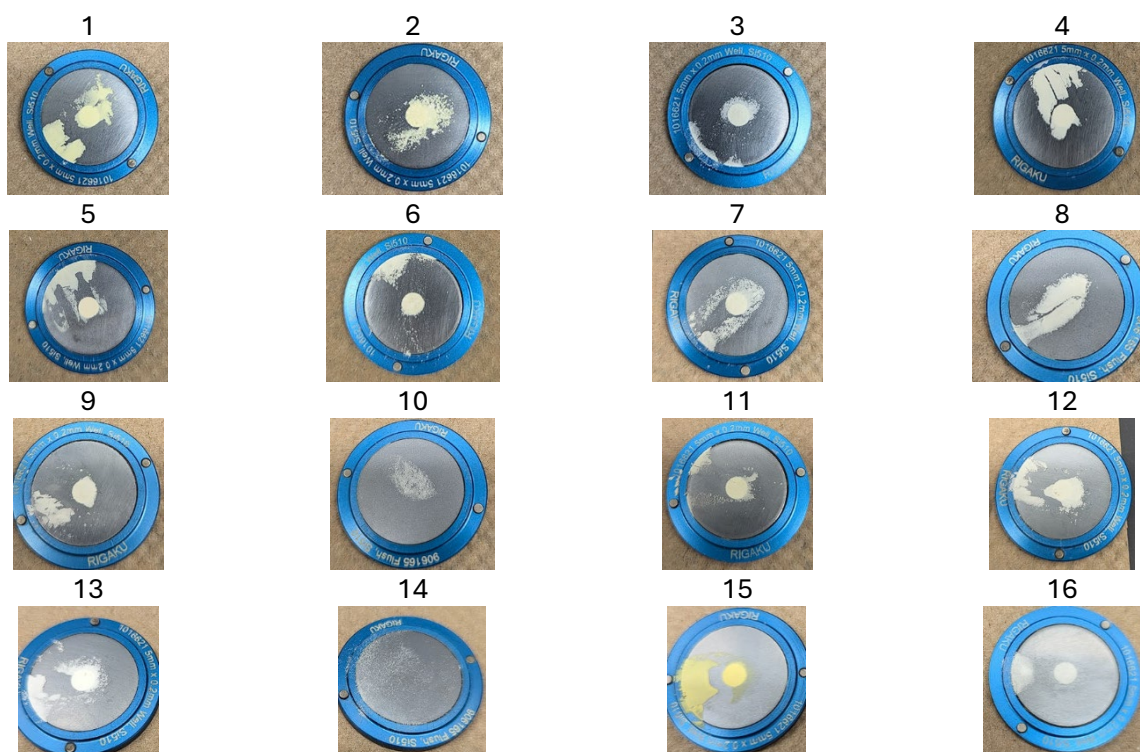


Figure S7 Pictures of Y-Uio-66 samples obtained from the 16 experiments of the DoE.

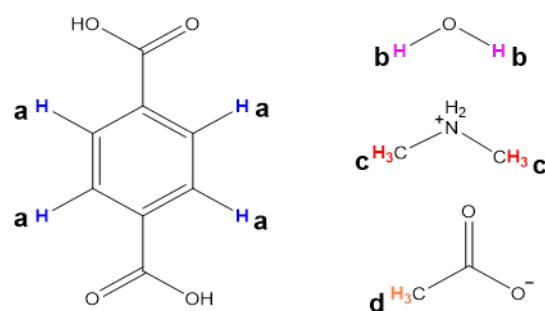
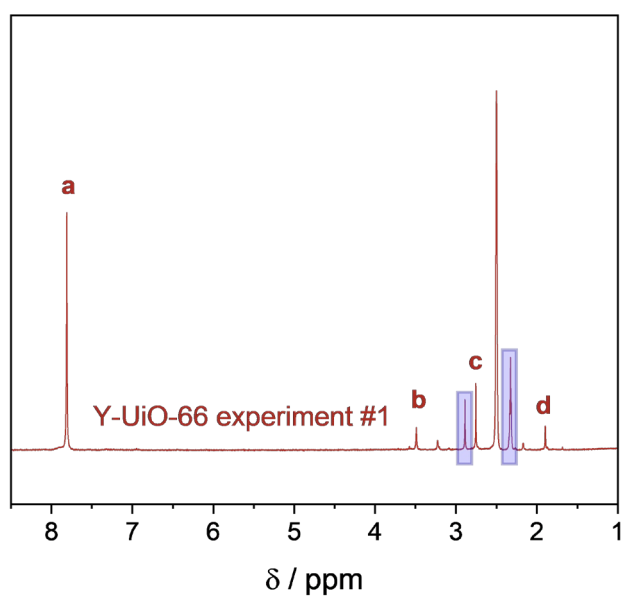


Figure S8  $^1\text{H}$  NMR spectrum of Y-Uio-66 obtained in experiment 1. Blue boxes indicate the peaks that do not correspond to the MOF. Solvent:  $\text{DMSO-d}_6$  (2.5 ppm), with  $\text{D}_2\text{SO}_4$  for digestion.

Table S2 Chemical shifts and integrations for the <sup>1</sup>H NMR spectrum in Figure S6.

H	δ (ppm)	Integration
BDC (Ha)	7.8	1.00
DMA (Hc)	2.8	0.19
Acetate (Hd)	1.9	0.10
Impurity 1	2.9	0.17
Impurity 2	2.3	0.52

Table S3 p-values obtained for each main factor by running the ANOVA of the design.

Factors	Lower Level (-1)	Higher Level (+)	Yield p-value	Surface area p-value
Temperature	120 °C	130 °C	$2.96 \times 10^{-3}$	$1.95 \times 10^{-10}$
Equivalents of modulator	16	20	0.0875	0.191
Equivalents of linker	1	1.4	0.0261	0.955
Time	24	48	$1.64 \times 10^{-3}$	$3.15 \times 10^{-7}$
Equivalents of co-modulator	9	13.5	0.538	0.0471
Volume of water	0.1 mL	0.2 mL	0.112	0.0984
Volume of solvent	4 mL	8 mL	0.0260	0.0382

Table S4 p-values obtained for eight interactions by running the ANOVA of the design.

Interaction	Yield p-value	Surface area p-value
Temperature*Modulator	0.0171	$3.06 \times 10^{-3}$
Temperature*Linker	0.538	$1.39 \times 10^{-4}$
Modulator*Linker	0.0111	$4.29 \times 10^{-3}$
Temperature*Time	$5.71 \times 10^{-7}$	0.0184
Modulator*Time	0.0676	0.0233
Linker*Time	0.538	0.0184
Time*Acid	$7.84 \times 10^{-4}$	0.378
Modulator*Linker*Time	0.0593	0.0670

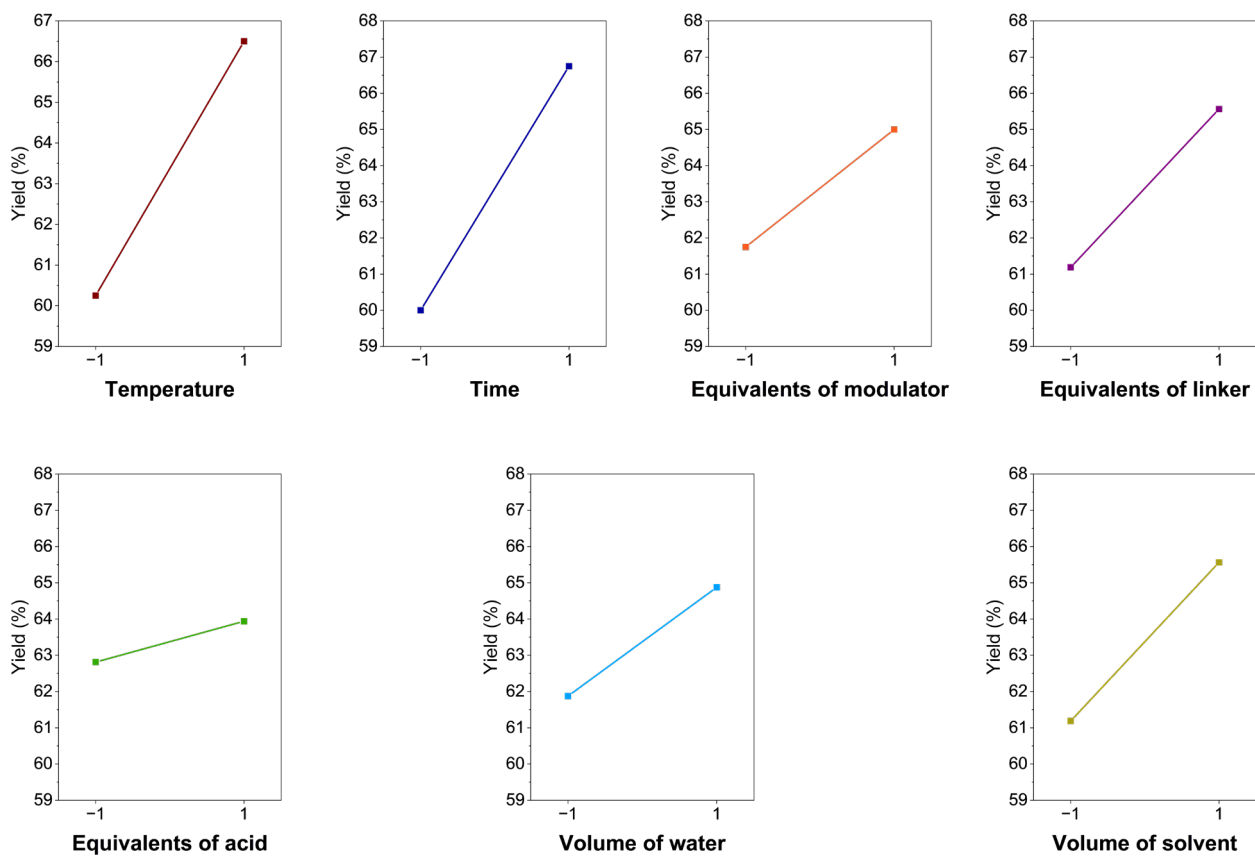


Figure S9 Main effects plots for yield

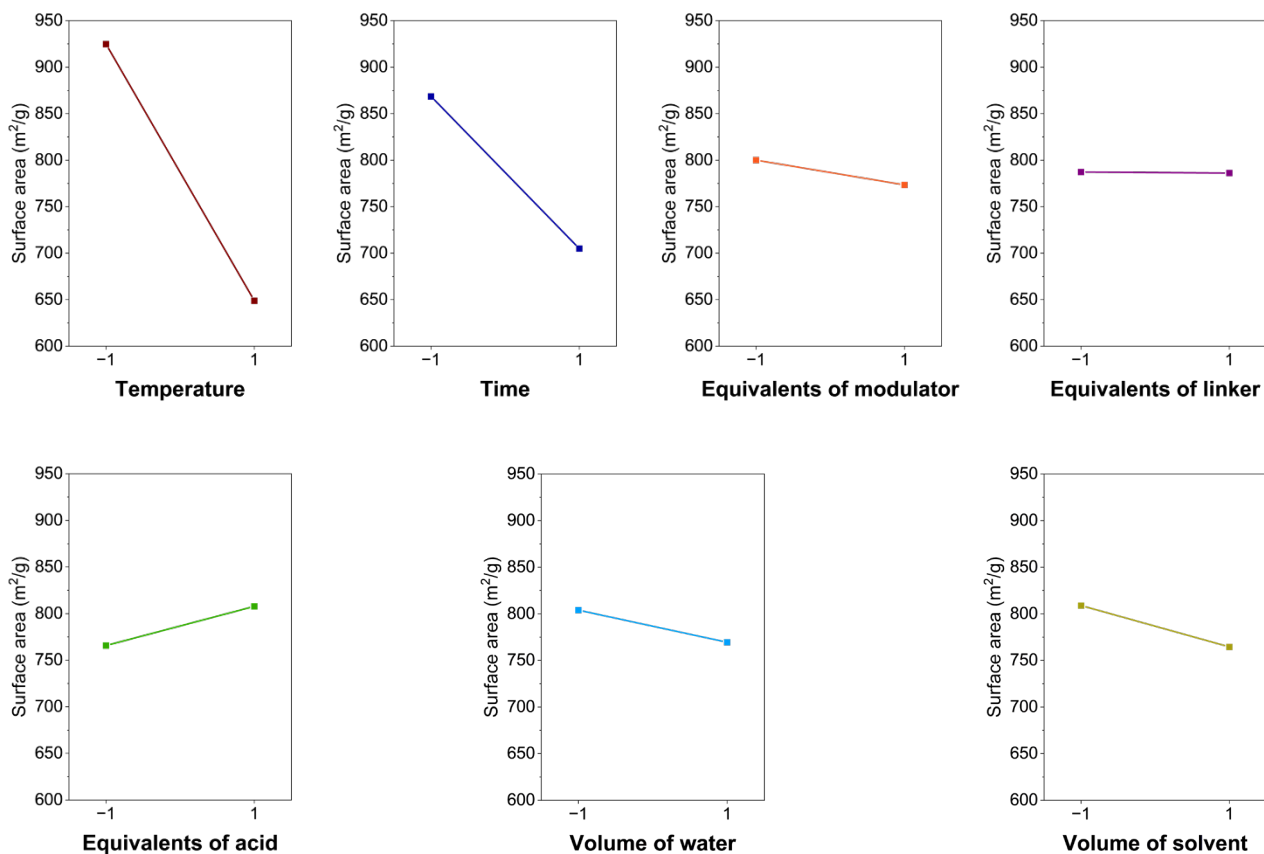


Figure S10 Main effects plots for surface area

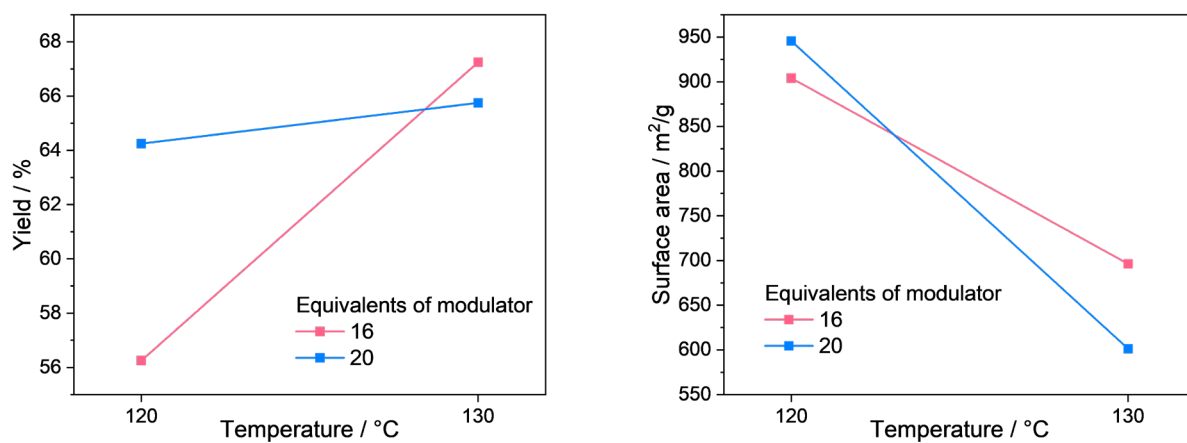


Figure S11 Interaction plots for Temperature\*Equivalents of modulator

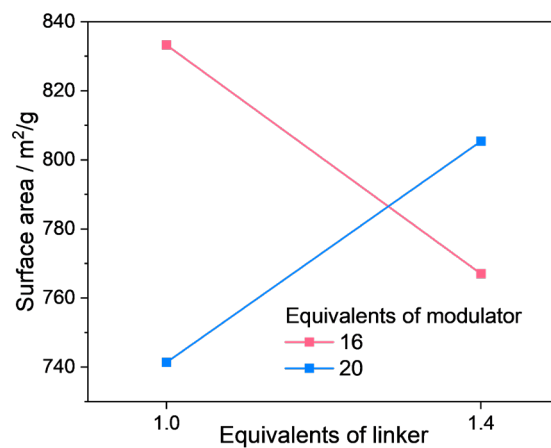
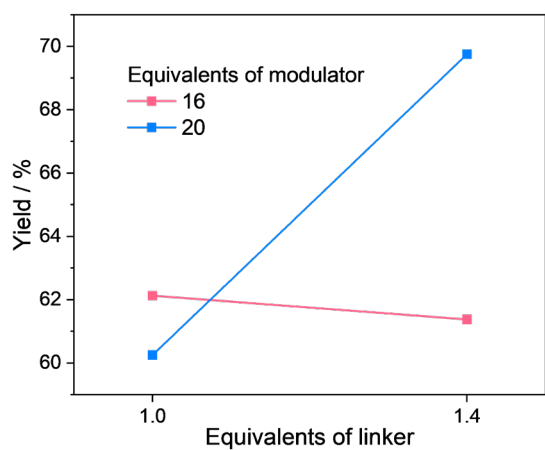


Figure S12 Interaction plots for Equivalents of linker\*Equivalents of modulator

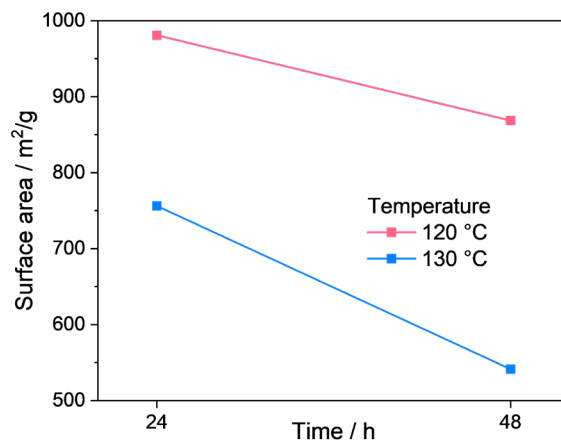
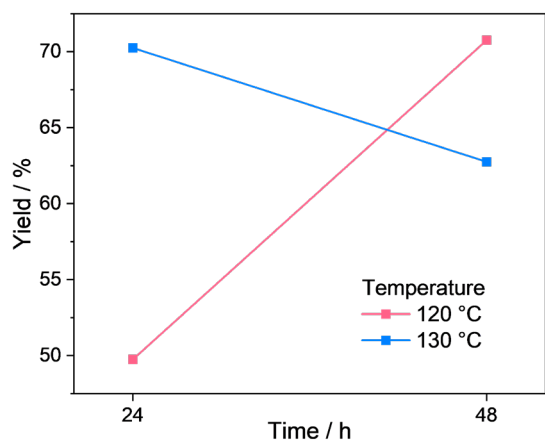


Figure S13 Interaction plots for Time\*Temperature



Figure S14 Pictures of Y-Uio-66 samples prepared using six optimized synthetic parameters and 4 (left) and 8 mL (right) of DMAc.

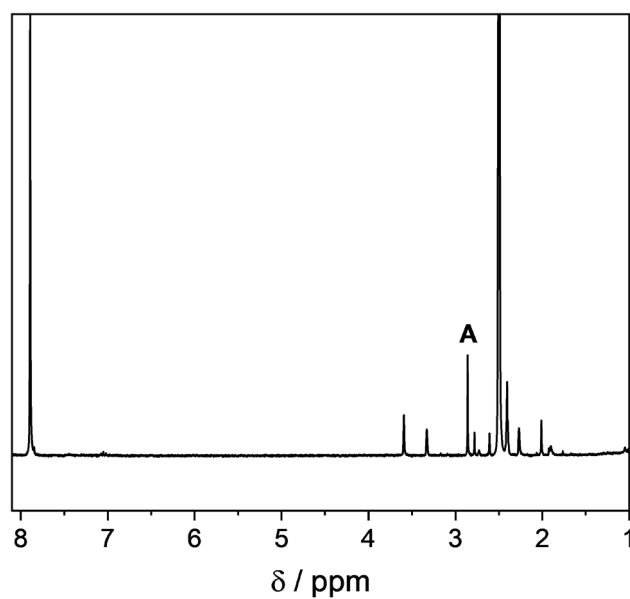


Figure S15  $^1\text{H}$  NMR spectrum of the 4 mL reaction after 3 washes with methanol, where peak A is the one observed in all the yellow samples.

Table S5 Yield and surface area of Y-UiO-66 sampled prepared using six optimized synthetic parameters and varying volume of DMAc solvent.

Solvent	Temperature	Modulator	Linker	Co-modulator	Water	Original			Duplicate		
						Yield (mg)	Yield (%)	Surface area ( $\text{m}^2/\text{g}$ )	Yield (mg)	Yield (%)	Surface area ( $\text{m}^2/\text{g}$ )
8 mL	120 °C	20 eq	1.4 eq	13.5 eq	0.2 mL	43.7	87	1030	40.5	81	1070
4 mL	120 °C	20 eq	1.4 eq	13.5 eq	0.2 mL	39.9	80	990	38.1	76	1080

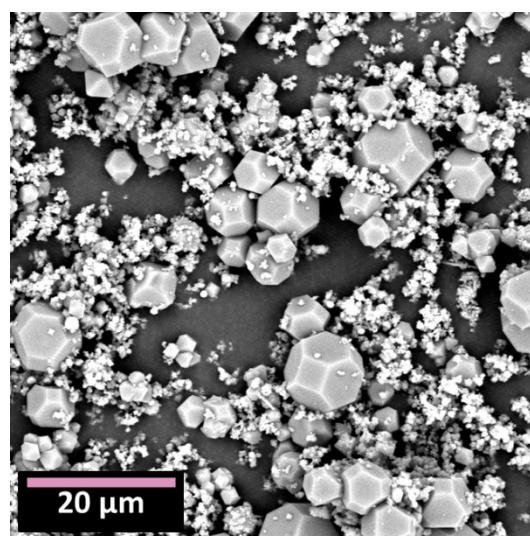
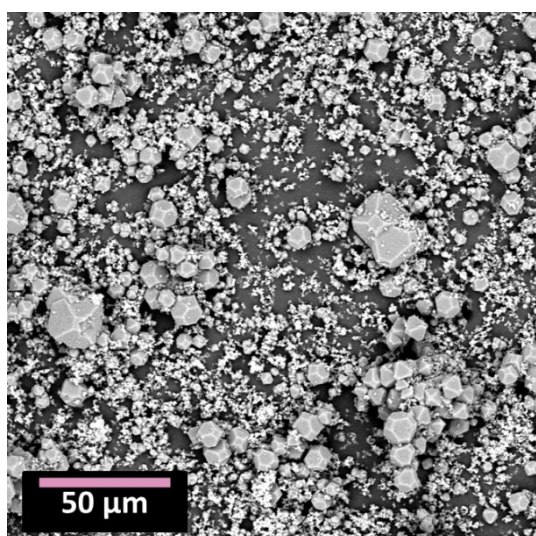


Figure S16 SEM images of Y-UiO-66 obtained using the optimized procedure

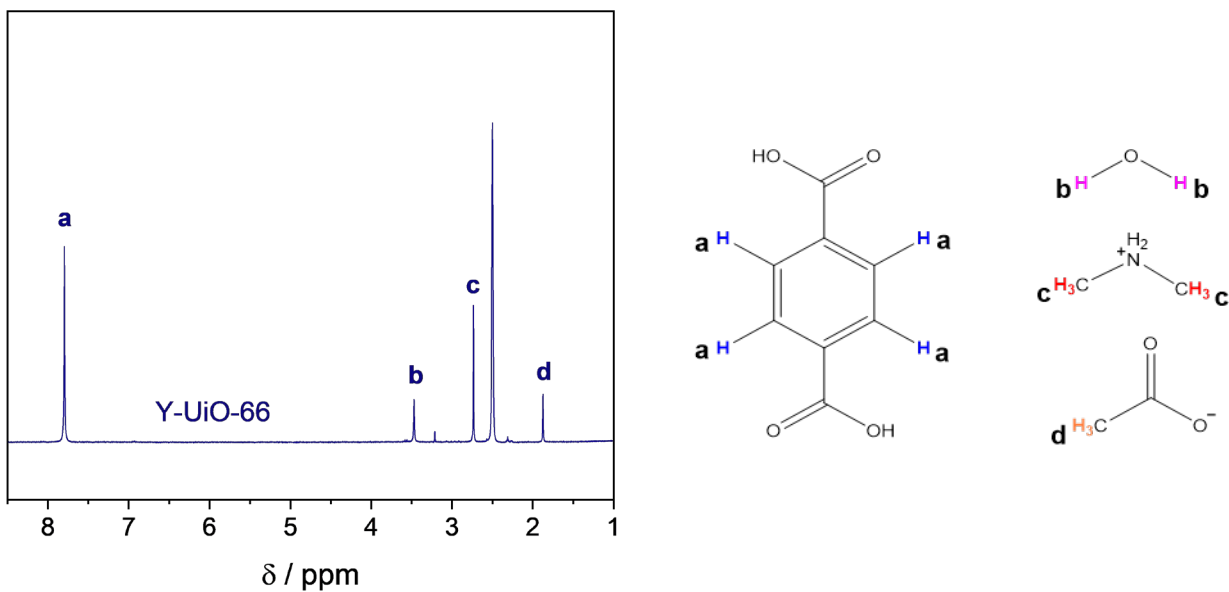


Figure S17  $^1\text{H}$  NMR spectrum of Y-UiO-66 obtained using the optimized procedure. Solvent: DMSO- $d_6$  (2.5 ppm), and  $\text{D}_2\text{SO}_4$  for digestion.

Table S6 Chemical shifts and integrations for the  $^1\text{H}$  NMR spectrum in Figure S14

H	$\delta$ (ppm)	Integration
BDC (Ha)	7.8	1.00
DMA (Hc)	2.8	0.39
Acetate (Hd)	1.9	0.19

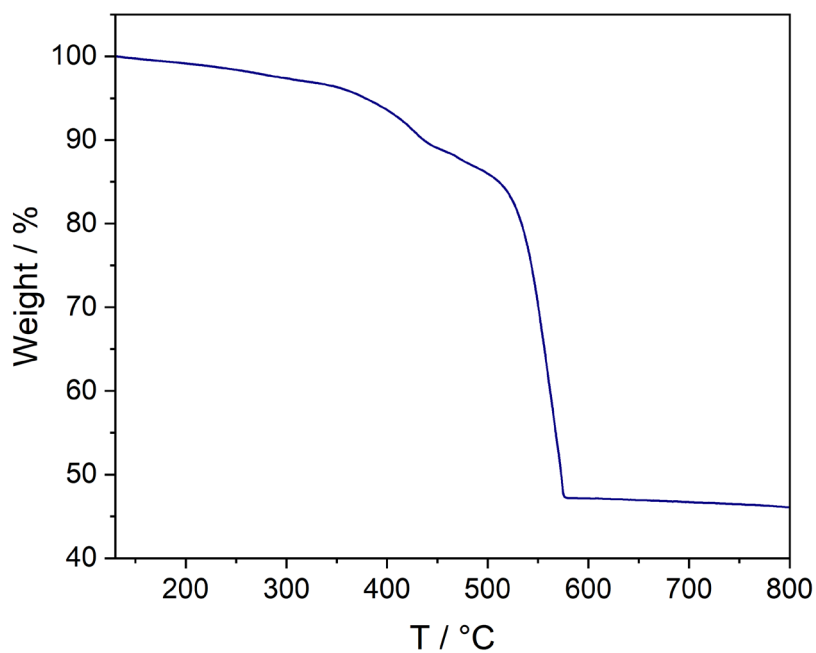


Figure S18 TGA of Y-UiO-66 obtained using the optimized procedure.

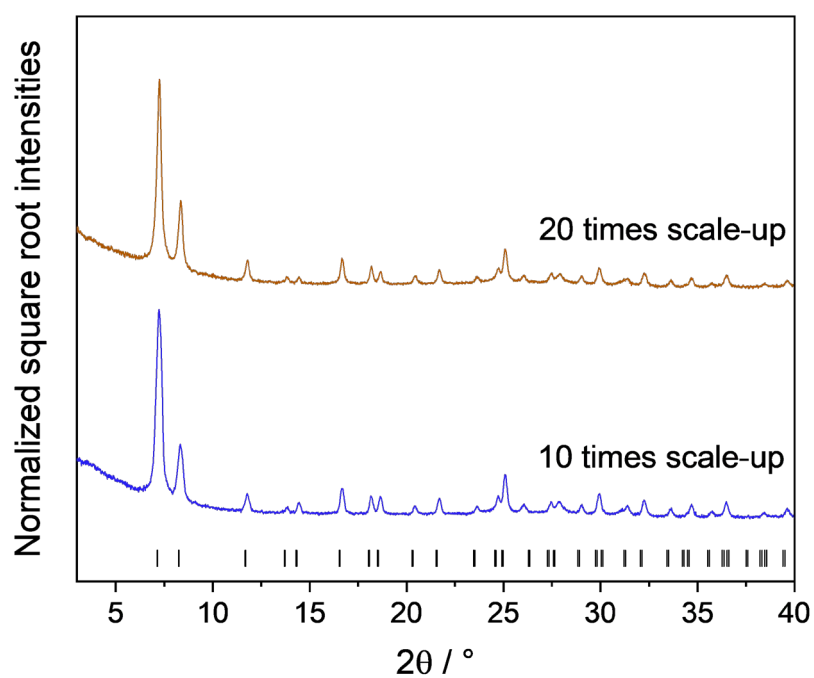


Figure S19 PXRD patterns of Y-Uio-66 samples obtained using the scaled-up procedures.

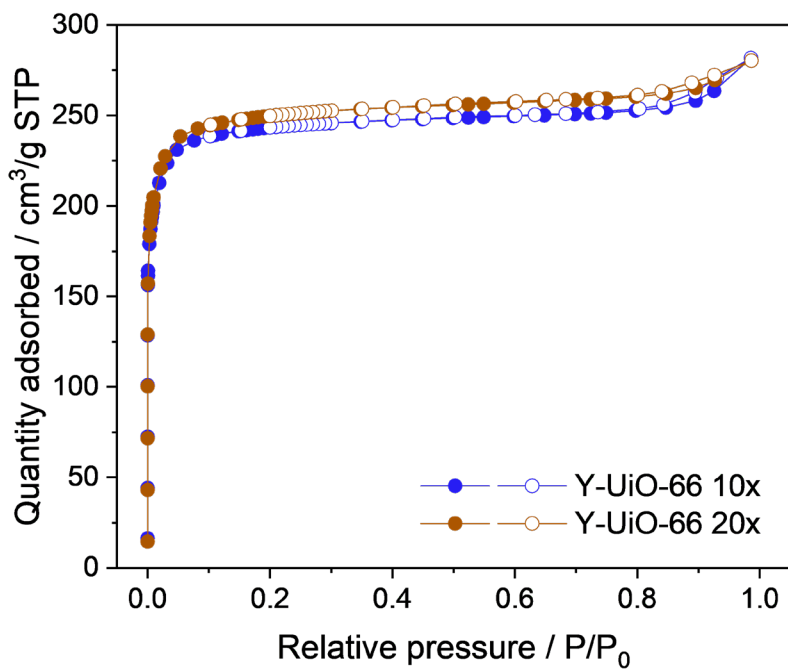


Figure S20 N<sub>2</sub> adsorption-desorption isotherms of Y-Uio-66 samples obtained using the scaled-up procedures. Closed circles correspond to adsorption and open correspond to desorption.

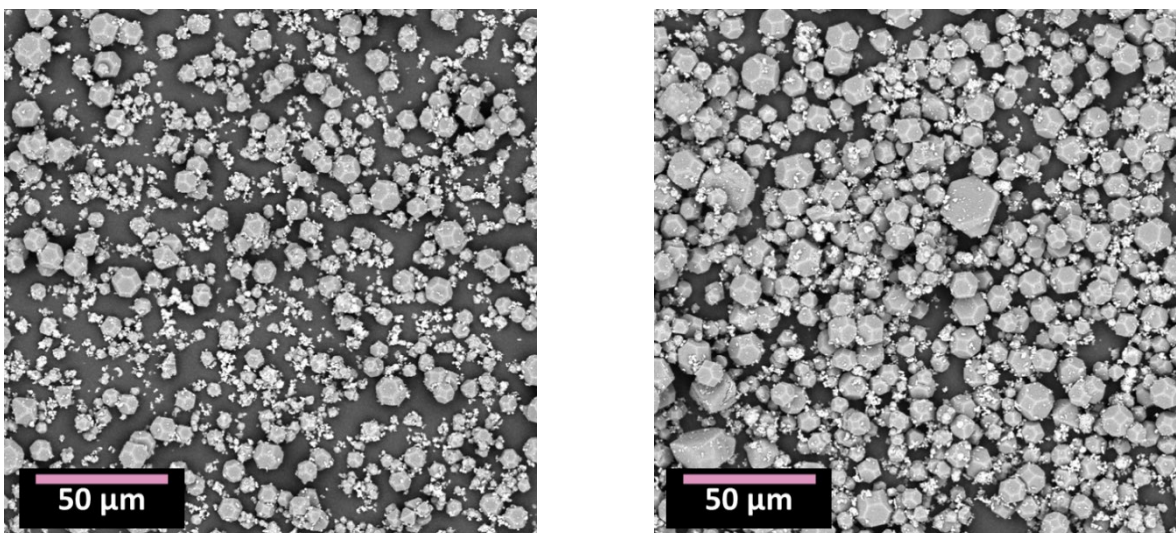


Figure S21 SEM images of Y-UiO-66 samples obtained using the scaled-up procedure 10x (left) and 20x (right).

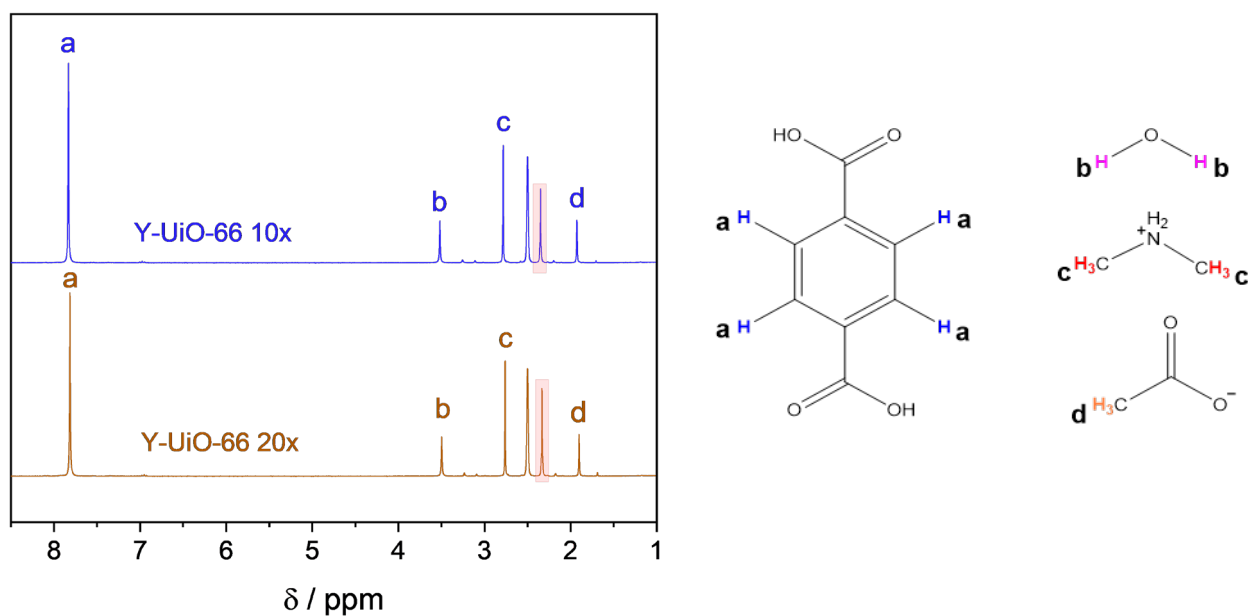


Figure S22  $^1\text{H}$  NMR spectra of Y-UiO-66 samples obtained using the scaled-up procedure before methanol washes. Red boxes indicate the peaks that do not correspond to the MOF. Solvent:  $\text{DMSO-d}_6$  (2.5 ppm), with  $\text{D}_2\text{SO}_4$  for digestion.

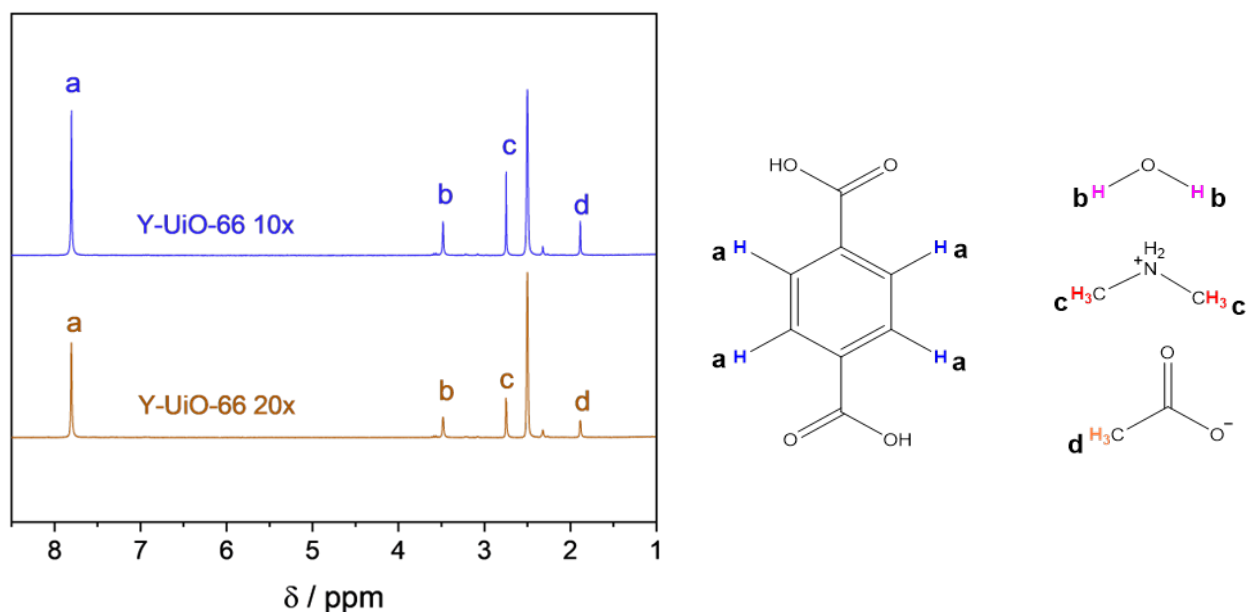


Figure S23  $^1\text{H}$  NMR spectra of Y-UiO-66 samples obtained using the scaled-up procedure after methanol washes. Solvent:  $\text{DMSO-d}_6$  (2.5 ppm), with  $\text{D}_2\text{SO}_4$  for digestion.

Table S7 Chemical shifts and integrations for the  $^1\text{H}$  NMR spectra in Figures S19 and S20.

H	$\delta$ (ppm)	Integrations			
		10x before MeOH	10x after MeOH	20x before MeOH	20x after MeOH
BDC (Ha)	7.8	1.00	1.00	1.00	1.00
DMA (Hc)	2.8	0.40	0.40	0.40	0.40
Acetate (Hd)	1.9	0.20	0.20	0.20	0.20
Impurity	2.3	0.34	0.06	0.40	0.09

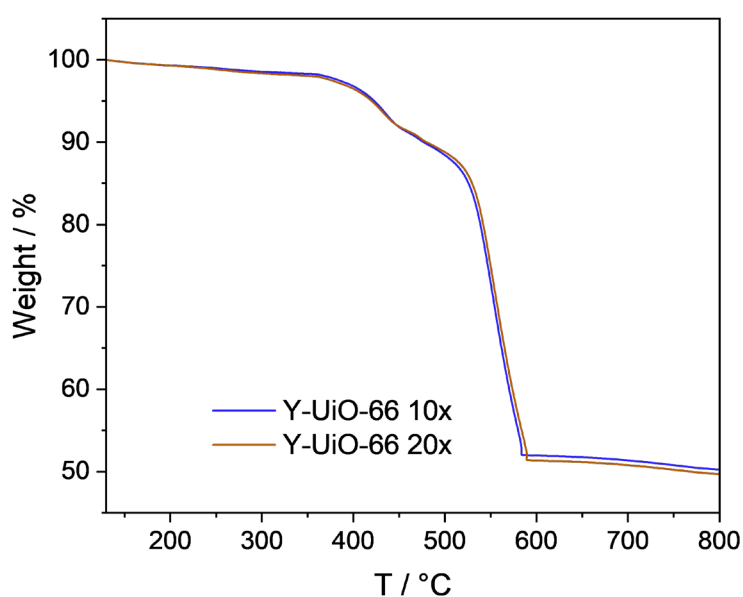


Figure S24 TGA for Y-UiO-66 samples obtained using the scaled-up procedure after methanol washes.

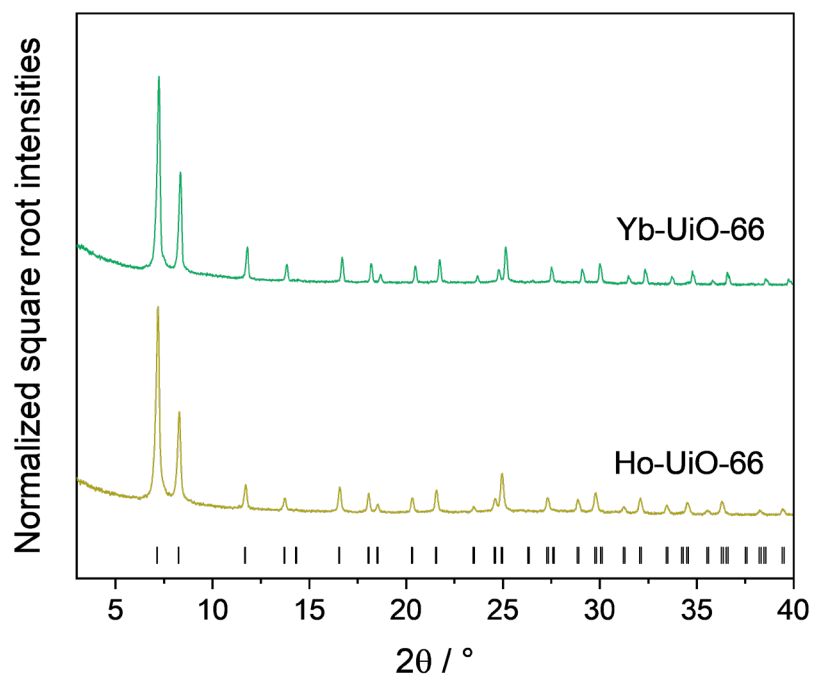


Figure S25 PXR D patterns of Ho-UiO-66 and Yb-UiO-66 samples synthesized using the newly optimized procedure based on the DoE results for Y-UiO-66.

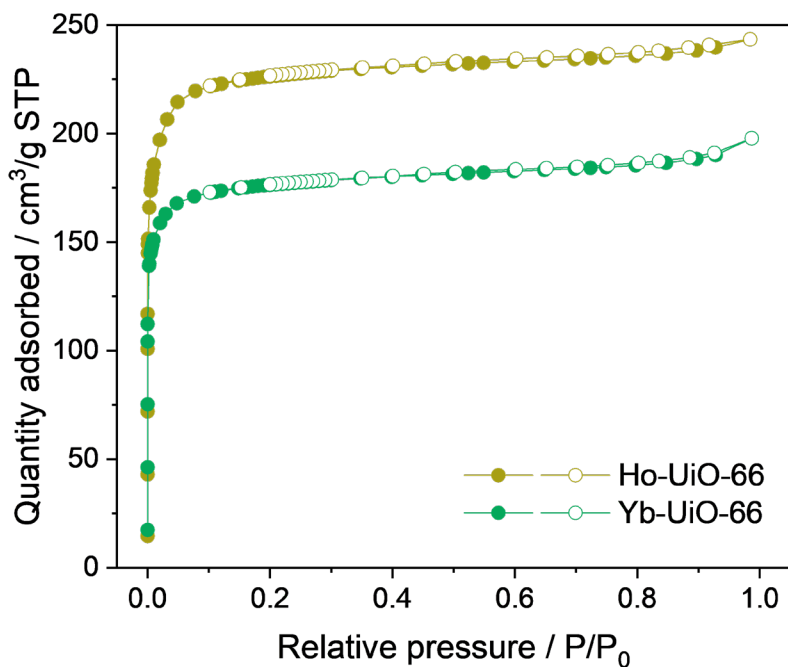


Figure S26 N<sub>2</sub> adsorption-desorption isotherms of Ho-UiO-66 and Yb-UiO-66 samples synthesized using the newly optimized procedure based on the DoE results for Y-UiO-66. Closed circles correspond to adsorption and open correspond to desorption.

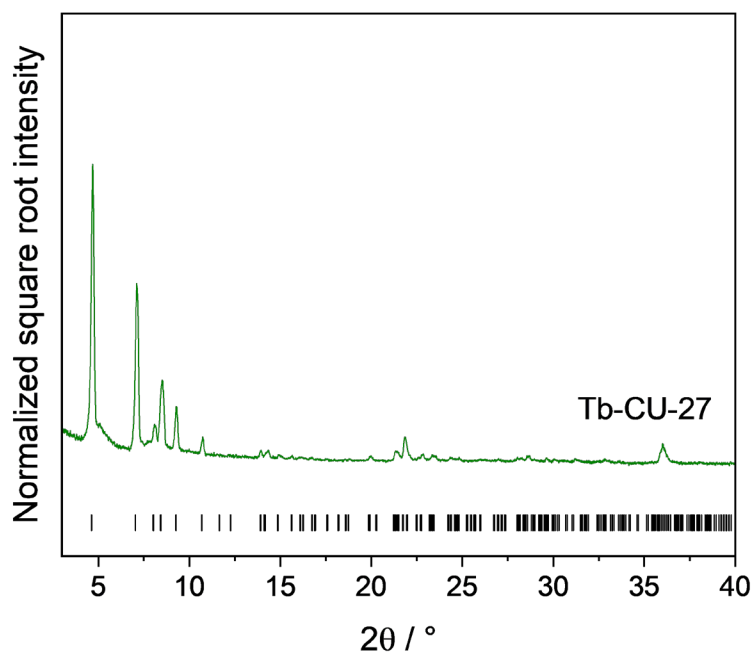


Figure S27 PXRD pattern of Tb-CU-27 synthesized using an optimized procedure adapted from the results obtained for the DoE for Y-UiO-66.

Table S8 Summary of the synthetic procedures to obtain RE-UiO-66

MOF	Yield (%)	Surface area (m <sup>2</sup> /g)	Reference
Y-UiO-66	Not reported	1360	2
Y-UiO-66	39	1060	3
Y-UiO-66	84	1050	This work
Ho-UiO-66	Not reported	1000	2
Ho-UiO-66	31	820	3
Ho-UiO-66	Not reported	790	4
Ho-UiO-66	88	890	This work
Yb-UiO-66	Not reported	1080	2
Yb-UiO-66	23	650	3
Yb-UiO-66	Not reported	700	4
Yb-UiO-66	82	700	This work

Reference 2 is the original procedure for the synthesis of RE-UiO-66. This report explores the synthesis in DMF, and how using a mixture of DMF:DMAc, or even DMAc alone, helps with reproducibility of the synthetic procedure. Furthermore, the addition of nitric acid is discussed with the same purpose. Reference 3 and 4 use the “best” procedure from the previous report (Reference 2) which is: 1 equivalent of linker, 16 equivalents of 2,6-dFBA, 8 mL of DMAc, 0.1 mL of water, 0.1 mL of nitric acid, 120 °C for 24 hours. This procedure leads to lower surface areas than the others reported in Reference 2, and the presence of dimethylammonium cations and acetate capping ligands is observed, suggesting a difference in the number of defects in the samples using this “best” procedure. Reference 3 also reports the use of RE acetates in place of RE nitrates for this “best” procedure, obtaining comparable results.

This work herein starts with the procedure from References 3 and 4, keeping the same reagents but improving the yield by varying their ratios and the reaction time.

## References

1. Balkus, K. J.; Mortensen, M. L.; Simin, S.; Vizuet, J. P., Defluorination of organo-fluorine molecules by rare-earth ions resulting in fluoro-bridged metal-organic frameworks. U.S. Patent Application No. 18/303,914.
2. P. R. Donnarumma, S. Frojmovic, P. Marino, H. A. Bicalho, H. M. Titi and A. J. Howarth, *Chem. Commun.*, 2021, 57, 6121-6124.
3. M. Richezzi, P. R. Donnarumma, C. Copeman and A. J. Howarth, *Chem. Commun.*, 2024, 60, 5173-5176.
4. P. R. Donnarumma, C. Copeman, M. Richezzi, J. Sardilli, H. M. Titi and A. J. Howarth, *Cryst. Growth Des.*, 2024, 24, 1619-1625.